

Article Info

Received : 2022-07-06 Accepted : 2022-07-28
 Revised : 2020-07-28 Available online : 2022-08-31

Photovoltaic (PV) thermal performance simulation using segmentation lapping fin passive cooling

Ahmad Yonanda^{1*}, Amrizal¹, Harmen¹, Akhmad Riszal¹, and Fauzi Ibrahim²

¹Department of Mechanical Engineering, Faculty of Engineering, University of Lampung, Bandar Lampung, 35143, Lampung, Indonesia.

²Department of Mechanical Engineering, Faculty of Engineering, University of Malahayati, Bandar Lampung, 35143, Lampung, Indonesia

* Corresponding author: ahmad.yonanda@eng.unila.ac.id

Abstract

The sun is a renewable energy source that has several advantages such as being easy to obtain, free of pollution, and available in sufficient quantities. The heat energy received by the photovoltaic can cause an increase in surface temperature, resulting in a decrease in electrical efficiency. One of the efforts to increase photovoltaic electrical efficiency is using air cooling, by adding absorber fins or thermal photovoltaic (PV/T). The lapping type fin has superior performance in reducing the temperature of the PV module compared to the linear (conventional) fin type. The purpose of this study was to compare the performance of thermal PV using conventional fins with lapping segmentation fins carried out using the CFD approach using ANSYS Fluent. The simulation test procedures include: making linear fin geometry (conventional), linear lapping and segmentation lapping, conducting mesh quality studies, and determining boundary conditions and modeling parameters. Modeling variations in the direction of airflow 0°, 15°, 30°, 45°, 60°, 75°, and 90°. The numerical simulation results show that the use of segmented lapping fins can reduce the PV surface temperature by 1.79 °C or about 4.11% compared to conventional (linear) lapping in the airflow direction of 90° (parallel to the fins). The results of this study support the use of integrated PV and passive cooling systems to reduce efficiency losses in actual conditions, where there is a multidirectional airflow characteristic, which may not be advantageous for conventional heatsinks.

Keywords:

Air cooling, fin lapping, thermal performance, photovoltaic, and simulation CFD

1 Introduction

The potential of renewable energy, such as solar energy, is energy that is actively being developed by the Indonesian government for now which is expected to reduce conventional energy consumption. To take advantage of solar energy, namely using Photovoltaic (PV) which will later be converted into electrical energy. The problem is that Photovoltaic is only able to convert solar radiation energy into electrical energy with an efficiency level of 12-18% and more than 80% where the energy can be converted or absorbed into heat energy [1].

An increase in temperature of 1°C in photovoltaic will result in a decrease in electrical efficiency of 0.5% [2,3]. The reduction in

excessive heat temperature in photovoltaics will result in high electrical efficiency [4,5]. Electrical efficiency can be maximized by applying suitable heat extraction with fluid circulation. This extracted heat can be used to heat air or water [6]. Several studies continue to be developed covering aspects of numerical modeling optimization [7], mass flow rate variations [8], steady state 1D, 2D, and 3D [9] types of working fluid flow, and economic aspects [10]

One of the efforts to increase the electrical efficiency of Photovoltaic is using air cooling, by adding absorber fins or Thermal Photovoltaic (PV/T). This method is a good way to increase photovoltaic efficiency. Proper photovoltaic module cooling techniques can increase the performance and life of the photovoltaic module. Many researchers prefer to use passive cooling techniques because they do not require additional power to operate [11]. Based on the passive cooling PV/T research conducted by [6] using the type of lapping fins and planner reflector, the result is that lapping fins have superior performance in reducing the temperature of the PV module compared to linear fins. Furthermore, it was found that the thickness of the designed aluminum fin above 2 mm showed no effect on the PV power and efficiency.

In experimental research that has been carried out by [12] i.e., two 250 W Photovoltaic modules are installed at a height of 37 cm from ground level to make room for air cooling. The results obtained are an increase in output power of 20.96 W with an increase in efficiency of not less than 3%. Then Photovoltaic cooling is based on the concept of evaporative cooling by using pin-shaped fins as heat sinks. The results of the research conducted by [13] showed that Photovoltaic efficiency and Photovoltaic output power increased to 31.5% and 32.7%, respectively, with a decrease in the temperature of the Photovoltaic module up to 20.05%. In addition, a study using a passive cooling system (fin) simulation method using the concept of Computational Fluid Dynamics (CFD) was developed by [14]. The simulation results show that the surface temperature of the Photovoltaic module and the electrical efficiency without cooling are found to be 62.78 °C and 13.24%, respectively. Meanwhile, by using fin cooling, the temperature drop of the photovoltaic module is 15.13 °C.

In addition [15] also carried out experimental and economic analysis of passive cooling PV modules using planar fins and reflector modules, showing that by using straight fins and lapping fins, the PV modules can be used for 4.2 and 5 years, respectively. Therefore, PV modules that use passive cooling techniques, especially lapping fin designs, are the best choice compared to straight fin designs because they are cheaper in terms of economy.

Based on the above review, most of the research that has been done in PV/T system design is by adding absorbent plates (fins) on the back of conventional PV panels because the increase in PV cell temperature causes a decrease in electrical efficiency. Designs with more efficient cooling methods can improve electrical and thermal efficiency. Based on the existing literature information, there are still few references that explain the changes in shape fin configuration on performance both for thermal and electrical resulting. In this study, the comparison of fin designs on PV panels related to changes in the shape of the fins is simulated with the CFD approach using ANSYS Fluent. Airflow direction modeling 0°, 15°, 30°, 45°, 6°, 75° dan 90° [12].

2 Research Methods

The research approach used is the PV/T performance simulation method using CFD software (Ansys Fluent version 21.2). The model in this study uses segmented lapping fins in the hope of maintaining consistent performance in conditions where wind flow and direction vary continuously according to environmental conditions in the Bandar Lampung area (Fig. 1).

This study also examines the effect of thermal on the shape of different scenarios including: without heatsink, with conventional heatsink, lapping heatsink, and multi-angle (segmented) heatsink.

study, the number of cells was 3,204,424 with a minimum orthogonal quality of 0.15 (Fig. 3).

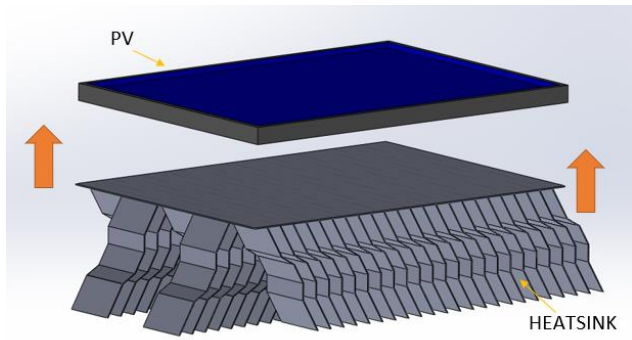


Fig. 1. PV cooling system representation.

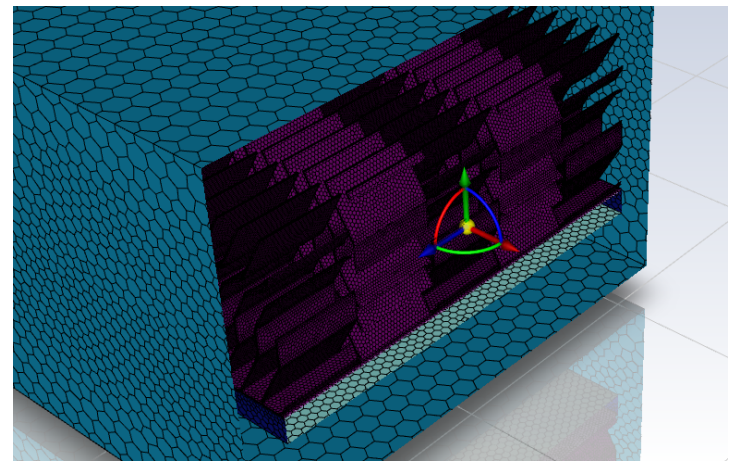


Fig. 3. Mesh type polyhedral.

2.1 Geometry Modeling

The geometric shape of the linear lapping and segmented fins can be seen in Fig. 1, respectively for the linear fins (Fig. 2.a.) and segmented fins (Fig. 2.b.) The dimensions are the same for the height (200 mm), fin spacing (Fig. 25.75 mm), and fin thickness (2 mm) while the dimensions of PV and flat plates as absorbers measure 665 x 500 mm². For segmented fins using a tilt angle of 30° to the Y axis, with a total of 5 fins per row and a total of 115 fins (Fig. 2.c.), the fin parameters can be seen in Table 1.

Table 1. Boundary conditions, heatsink parameters, and PV module.

Boundary conditions	Value
Solar irradiance	1000 W/m ²
Ambient temperature	30 °C
Wind direction	0, 15, 30, 45,60, 75, 90 °
Wind speed	2 m/s
Front Surface emissivity	0.8
Fin length	200 mm
Fin width	500 mm, 100 mm
Fin number per row	1 fin, 5 fins
Fin spacing	25.75 mm
Fin angle	0°, 30° with Y axis
Sheet gauge (fin thickness)	2 mm

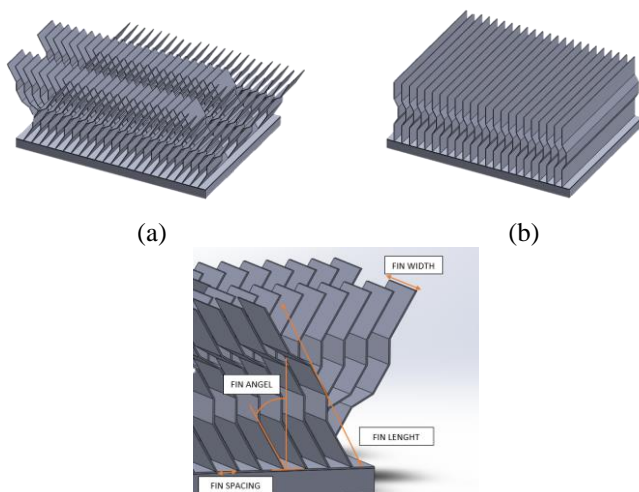


Fig. 2. PV cooling system (a), lapping heatsink, (b) segmentation heatsink, and (c) fin parameters.

2.2 Modeling mesh

To get a structured mesh for easy iteration, the procedure is applied by making a local sizing of the fin area of 2 mm, then the size function uses a curvature with a polyhedral mesh type. In this

2.3 Computational modeling

Heat transfer in air-cooled PV modules includes numerous strong and fluid spaces. The liquid space incorporates the functioning liquid fenced-in area of the PV module + heatsink, which is likewise present in the heatsink. The physical aspects of fluids are governed by the following principles: conservation of mass, conservation of moment, and conservation of energy. These principles can be expressed in terms of the Navier-Stokes equation (Eq. 1-3):

Continuity:

$$\frac{\partial \rho}{\partial t} + \nabla \cdot (\rho \vec{v}) = 0 \quad (1)$$

Moment:

$$\frac{\partial}{\partial t} (\rho \vec{v}) = -\nabla p + \nabla \cdot (\vec{\tau}) + \rho \vec{g} \quad (2)$$

Energy:

$$\frac{\partial}{\partial t} (\rho E) + \nabla \cdot (\vec{v} \cdot (\rho E + p)) = -\nabla \cdot \left(\sum_j h_j J_j \right) \quad (3)$$

Where ρ is density, τ is tensor stress, p is static pressure, v is velocity, E represents energy, h is the enthalpy of species, and J is diffusion flux. The governing equations are discretized using the standard finite volume method to form a system of algebraic equations that are solved by an iterative process using Computer Fluid Dynamics software.

Meanwhile, the turbulent kinetic energy is given by (Eq. 4):

$$\frac{\partial}{\partial t} (\rho k) + \frac{\partial}{\partial x_i} (\rho k u_i) = \frac{\partial}{\partial x_j} \left(\alpha_k \mu_{eff} \frac{\partial k}{\partial x_j} \right) + G_k - \rho \epsilon \quad (4)$$

where G_k represents the generation of turbulent kinetic energy due to the mean velocity gradient, α_k and α_ϵ are the reciprocal of the Prandtl values for k and ϵ .

2.4 Simulation setup

This simulation test uses steady-state conditions. In addition, several boundary conditions are given in this stage, including the fluid flow velocity in the channel is 2 m/s (constant) and heat losses at the bottom of the collector are ignored [15]. The computational domain consists of a fluid boundary box (enclosure) of 865 mm x 600 mm x 230 mm which envelope a photovoltaic + heatsink (see Fig. 4). The photovoltaic geometry consists of 5 sections consisting of the properties of standard PV module coatings (Table 2).

Table 2. Thermo-physical properties of the PV model domains

Domain	Thickness (mm)	Thermal Conductivity (W/m °K)	Density (kg/m ³)	Specific heat (J/kg °C)
Low-iron glass	3	1.8	3000	500
Cell	0.31	148	2331	677
EVA	0.52	0.353	960	2090
Tedlar	0.13	0.21	1200	1250
Aluminum	0.71	202.41	2719	871

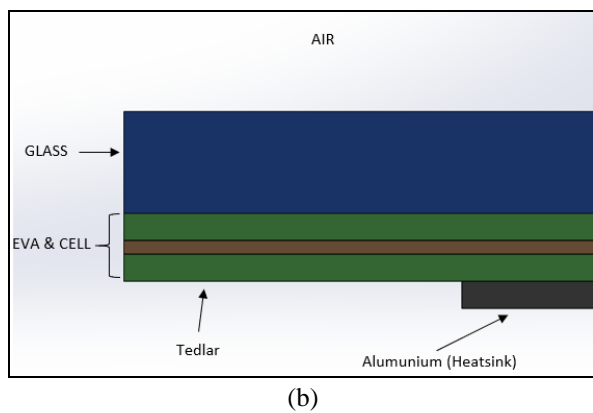
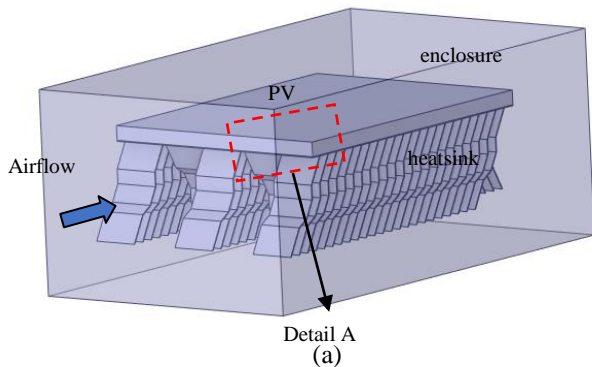


Fig. 4. (a) Computing domain and (b) standard coating

Meanwhile, in the last stage, the final results of the simulation process are presented by displaying color contours and graphics to make it easier for further analysis. For more details, it can be seen in the simulation flow as given in Fig. 5.

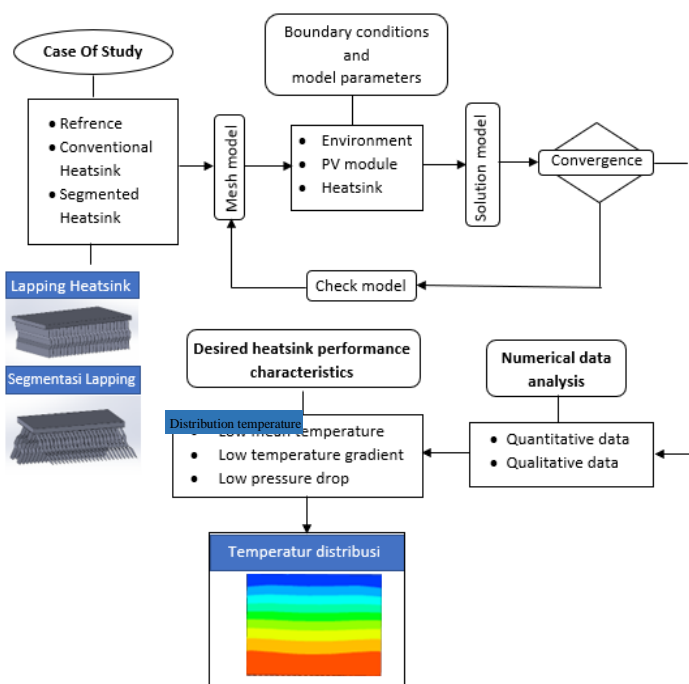


Fig. 5. PV/T performance simulation process schematic

3 Results and Discussion

Previous research [16] Ansys software validation has been carried out by comparing the results of simulation tests with experimental data, it is found that there is a closeness of the correction factor values which tend to be the same between the simulation results and the experimental data. Thus, the simulation software used can be relied upon to predict the thermal characteristics of the collector.

3.1 Thermal effect of type heatsink

The simulation results of photovoltaic (PV) thermal performance can be seen in Table 3 which shows 4 variations of the test, each evaluated from 7 airflow directions (0°, 15°, 30°, 45°, 60°, 75°, and 90°). The surface temperature of the PV varies according to the direction of the airflow.

Table 3. Summary of simulation numerical results (mean PV surface temperature)

Heatsink	Temperature surface PV(°C)		Temperature reduction(%)	
	Best case	Wort case	Best case	Wort case
No heatsink	47.72	50.00	0	0
conventional	44.43	47.88	6.89	4.24
conventional Lapping	43.55	47.65	9.38	4.90
Segmented	41.76	45.89	13.68	8.62

The observed temperatures are the lowest for the best case to the highest for the worst case. From the general simulation test results, the temperature is lower when the air flows at 90° (perpendicular to the fins), and higher when the airflows at 0° (parallel to the fins). With using temperature segmentation lapping fins the maximum reduction obtained is around 5.96 °C (13.68%) compared to without using fins (no heatsink) while 1.79 °C (4.11%) compared to conventional lapping fins.

The temperature distribution of this surface which can be seen in full in Fig. 6 has the same trend as the temperature distribution of the PV surface in the airflow direction of 45°, with and without fins. PV dimensions of 665 x 500 mm², which was used as the geometric parameter for this study.

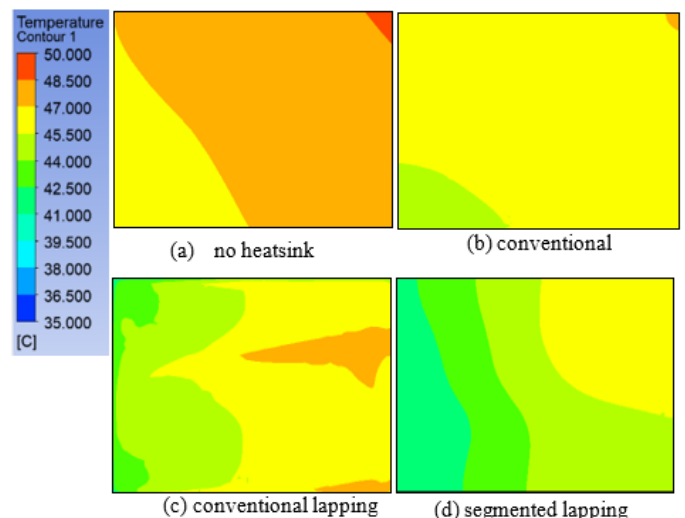


Fig. 6. Temperature distribution of PV using different types of heatsink

3.2 Effect of airflow direction

In Fig. 7, the type of lapping segmentation fin shows better performance compared to PV without fins or using conventional fins, especially when the air velocity is 2 m/s with the airflow direction approaching 90° (parallel to the fins). This is certainly expected to produce better electrical efficiency.

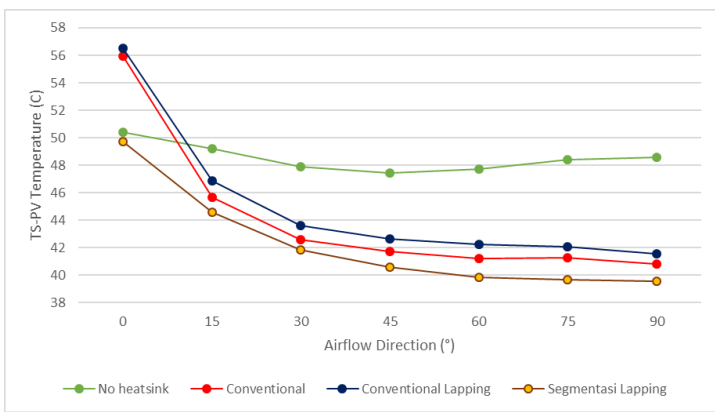


Fig. 7. heatsink comparison for variation air flow of pressure drop

This lower surface temperature in terms of equation (4) may be caused by the shape of the fins that produce turbulent flow so that it will increase the Nusselt number [12].

Thus, there is an increase in the rate of heat transfer which is characterized by an increase in the difference in surface temperature of the PV panels between conventional and segmented slabs. For each simulated flow direction (0°, 15°, 30°, 45°, 60°, 75°, and 90°), the average surface temperature of PV produced using conventional lapping fins is 56.51 °C, 46.87 °C, 43.58 °C, 42.66 °C, 42.26 °C, 42.04 °C, and 41.54 °C, for the lapping segmentation fins are 49.7 °C, 44.60 °C, 41.86 °C, 40.57 °C, 39.86 °C, 39.65 °C dan 39.56 °C.

3.3 Pressure Drop Effect of type heatsink

When the air flows parallel to the fins (90°), the pressure drop is very minimal for all types of fin models, namely: conventional, lapping, and segmented fins (Fig. 8). The segmentation fin allows for slightly increased turbulence resulting in a greater reduction in temperature when compared to conventional geometries.

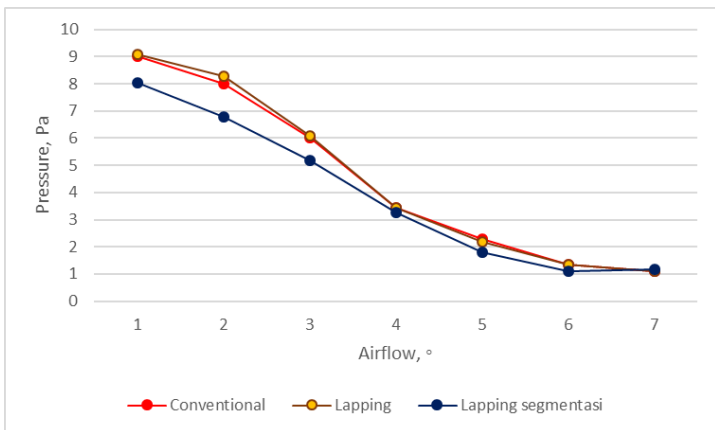
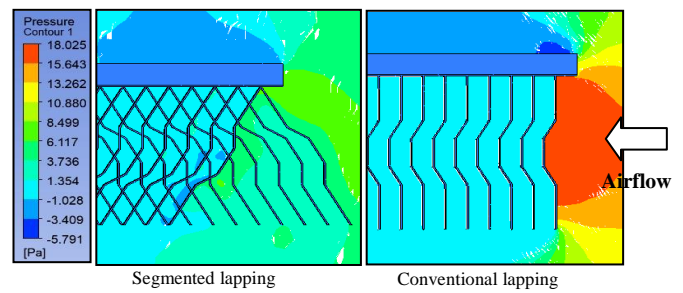


Fig. 8. heatsink comparison for variation airflow

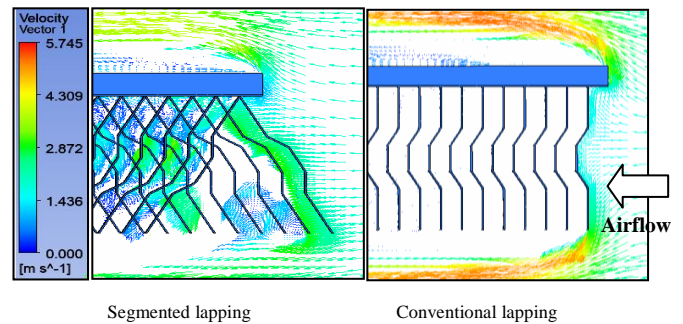
If the airflow is diagonal or angular (15°, 30°, 45°, 60°, 75°), all three fins show the same inclination trend. But the segmented fins allow airflow to pass through the gaps between the fins resulting in lower pressure drop and better heat transfer. The most significant case occurs when the airflow is perpendicular to the fin channel (0°). In this case, it deserves further analysis considering it is the scenario worst for all three fins, because the pressure drop is very high, especially for conventional heatsinks (Fig. 9).

A working fluid will experience a large pressure drop when flowing through a heat exchanger or fin (depending on the type of working fluid). The problem is that if the pressure drop is too large, there will be non-uniformity in the airflow, which adversely affects the heat transfer that occurs. Fig. 9.a. shows a comparison of the pressure contours in the 0° airflow direction. Lapping segmentation fins produce lower pressure drop than lapping fins (conventional) because they have a design that allows airflow to

pass through the gaps in the fins so that it will result in better interaction of the fluid with the dissipation surface.



(a)



(b)

Fig. 9. fins flow field with airflow at 0° (perpendicular to fin channels), (a) fins pressure distribution, (b) fins velocity distribution

In Fig. 9.b. the velocity distribution is observed around the fins. In the lapping fin, the segmentation shows a larger vortex flow within the fin, as well as a more gradual decrease in air velocity (more uniform flow). In contrast, conventional lapping fins produce a fluid flow that leads out of the fin channel so that the heat transfer contact is not optimal. In general, it is observed that the thermal performance of the fins has a high correlation with its hydraulic performance. When viewed from the design of the heatsink, the lapping segmentation type is much more economical. Dimension optimization is required to improve the performance of PV systems that are affected by high temperatures. This type of lapping segmentation is proven to be more efficient than conventional.

4 Conclusion

In this study, the performance of different fin shapes was tested using numerical simulations. It was found that the performance of conventional lapping fins can be improved under unfavorable weather conditions using the fins being segmented and bent by 30° from the Y axis, without increasing the material usage. The fin segmentation design is potentially more cost-effective, by optimizing the dimensions required to increase the performance of a PV system affected by high temperatures. By using lapping fin segmentation, the maximum temperature reduction obtained is about 5.96 °C (13.68%) compared to without using fins (no heatsink) while 1.79 °C (4.11%) compared to conventional lapping fins. Keeping the PV panels operating near STC (Standard Test Conditions) at 25 °C, can then extend the service life of PV, which is exposed to direct solar radiation for a longer period.

References

[1] N. Amrizal, D. Chemisana, J. I. Rosell, and J. Barrau, "A dynamic model based on the piston flow concept for the thermal characterization of solar collectors," *Appl. Energy*, vol. 94, pp. 244–250, Jun. 2012, doi: 10.1016/j.apenergy.2012.01.071.

- [2] N. Amrizal, D. Chemisana, and J. I. Rosell, "Hybrid photovoltaic–thermal solar collectors dynamic modeling," *Appl. Energy*, vol. 101, pp. 797–807, Jan. 2013, doi: 10.1016/j.apenergy.2012.08.020.
- [3] J. Deng *et al.*, "Validation of a simple dynamic thermal performance characterization model based on the piston flow concept for flat-plate solar collectors," *Sol. Energy*, vol. 139, pp. 171–178, Dec. 2016, doi: 10.1016/j.solener.2016.09.040.
- [4] S. Abdul Hamid, M. Yusof Othman, K. Sopian, and S. H. Zaidi, "An overview of photovoltaic thermal combination (PV/T combi) technology," *Renew. Sustain. Energy Rev.*, vol. 38, pp. 212–222, Oct. 2014, doi: 10.1016/j.rser.2014.05.083.
- [5] G. Kumaresan, P. Sudhakar, R. Santosh, and R. Velraj, "Experimental and numerical studies of thermal performance enhancement in the receiver part of solar parabolic trough collectors," *Renew. Sustain. Energy Rev.*, vol. 77, pp. 1363–1374, Sep. 2017, doi: 10.1016/j.rser.2017.01.171.
- [6] A. M. Elbreki, K. Sopian, A. Fazlizan, and A. Ibrahim, "An innovative technique of passive cooling PV module using lapping fins and planner reflector," *Case Stud. Therm. Eng.*, vol. 19, p. 100607, Jun. 2020, doi: 10.1016/j.csite.2020.100607.
- [7] A. E. Boubekri *et al.*, "Effects of Cr substitution on the low temperature magnetization behavior in amorphous Fe₆₈+Cr₁₂-Si₈B₁₂ ribbons," *J. Non-Cryst. Solids*, vol. 551, p. 120437, Jan. 2021, doi: 10.1016/j.jnoncrysol.2020.120437.
- [8] S. S. Moy, "Response to the letter by Dubey et al. (2013)," *Neurotoxicol. Teratol.*, vol. 41, p. 97, Jan. 2014, doi: 10.1016/j.ntt.2013.10.006.
- [9] H. A. Zondag, R. de Boer, S. F. Smeding, and J. van der Kamp, "Development of industrial PCM heat storage lab prototype," *Energy Procedia*, vol. 135, pp. 115–125, Oct. 2017, doi: 10.1016/j.egypro.2017.09.495.
- [10] "main - A new passive PV heatsink design to reduce efficiency losses A.pdf."
- [11] M. Hasanuzzaman, A. B. M. A. Malek, M. M. Islam, A. K. Pandey, and N. A. Rahim, "Global advancement of cooling technologies for PV systems: A review," *Sol. Energy*, vol. 137, pp. 25–45, Nov. 2016, doi: 10.1016/j.solener.2016.07.010.
- [12] J. G. Hernandez-Perez, J. G. Carrillo, A. Bassam, M. Flota-Banuelos, and L. D. Patino-Lopez, "Thermal performance of a discontinuous finned heatsink profile for PV passive cooling," *Appl. Therm. Eng.*, vol. 184, p. 116238, Feb. 2021, doi: 10.1016/j.applthermaleng.2020.116238.
- [13] J. Kim and Y. Nam, "Study on the Cooling Effect of Attached Fins on PV Using CFD Simulation," *Energies*, vol. 12, no. 4, p. 758, Feb. 2019, doi: 10.3390/en12040758.
- [14] T. Wongwuttanasatian, T. Sarikarin, and A. Suksri, "Performance enhancement of a photovoltaic module by passive cooling using phase change material in a finned container heat sink," *Sol. Energy*, vol. 195, pp. 47–53, Jan. 2020, doi: 10.1016/j.solener.2019.11.053.
- [15] A. M. Elbreki, A. F. Muftah, K. Sopian, H. Jarimi, A. Fazlizan, and A. Ibrahim, "Experimental and economic analysis of passive cooling PV module using fins and planar reflector," *Case Stud. Therm. Eng.*, vol. 23, p. 100801, Feb. 2021, doi: 10.1016/j.csite.2020.100801.
- [16] A. Yonanda, "Karakteristik Kolektor Surya Pelat Datar Aliran Spiral Menggunakan Metode Simulasi CFD," vol. 01, no. 01, p. 14, 2021.